Nuclear Instruments and Methods in Physics Research B 273 (2012) 270–273

Contents lists available at SciVerse ScienceDirect

Nuclear Instruments and Methods in Physics Research B

journal homepage: www.elsevier.com/locate/nimb

On the surface mapping using individual cluster impacts

F.A. Fernandez-Lima [a,*], M.J. Eller [a], J.D. DeBord [a], S.V. Verkhoturov [a], S. Della-Negra [b], E.A. Schweikert [a]

[a] Department of Chemistry, Texas A&M University, College Station, TX 77940-3012, United States
[b] Institut de Physique Nucléaire d'Orsay, Université Paris-Sud 11, CNRS/IN2P3, F-91406 Orsay, France

ARTICLE INFO

Article history:
Available online 27 July 2011

Keywords:
Photon emission
Electron emission
Secondary ion yield
Cluster-SIMS

ABSTRACT

This paper describes the advantages of using single impacts of large cluster projectiles (e.g., C_{60} and Au_{400}) for surface mapping and characterization. The analysis of co-emitted time-resolved photon spectra, electron distributions and characteristic secondary ions shows that they can be used as surface fingerprints for target composition, morphology and structure. Photon, electron and secondary ion emission increases with the projectile cluster size and energy. The observed, high abundant secondary ion emission makes cluster projectiles good candidates for surface mapping of atomic and fragment ions (e.g., yield >1 per nominal mass) and molecular ions (e.g., few tens of percent in the $500 < m/z < 1500$ range).

The performance of SIMS for molecular analysis has been notably enhanced with large cluster projectiles, e.g., C_{60} and Au_{400} [1–3]. However for surface imaging purposes, the use of cluster beams has some disadvantages when compared to mono-atomic and poly-atomic beams (e.g., Cs, Au_{1-3}, Bi_{1-3}, etc.). For example, a C_{60} beam is constrained by limitations in source brightness; in the case of massive clusters, e.g. Au_{400}, from liquid metal ion sources (Au-LMIS), their energy and angular emission are incompatible with tight focusing. In the present paper, we describe the potentialities of surface mapping by using spatially and temporally isolated events of individual projectile impacts for the case of C_{60} or Au_{400} projectiles. In particular, we present their advantage for surface molecule characterization, via electron emission microscopy (EEM), combined with the detection of secondary ions, SIs, and of photons emitted from a single cluster impact.

An experimental setup that comprises a cluster primary ion beam, an electron emission microscope, a photon detector and a ToF mass spectrometer was used for this study (Fig. 1). Two primary ion beams were used: (i) massive gold projectiles (e.g., Au_{400}^{+4}) from a Au-LMIS installed in a100 kV Pegase Platform and (ii) $C_{60}^{+1,2}$ from a 15 kV in-house-built effusion source [4,5]. The primary ion projectiles are massselected using a Wien filter and focused into the analysis chamber. To achieve the single event analysis mode, the primary ions were pulsed and/or collimated so that experiments were performed at <500 Hz. Emitted photons, electrons and secondary ions were collected per projectile impact. A photomultiplier (PMT, R4220P model from Hamamatsu Photonics), with an active window from 185 to 710 nm and a maximum 22% detection efficiency at 410 nm, was positioned behind the target for photon detection. Electrons emitted per impact were accelerated and then deflected using a weak magnetic field toward an electron emission microscope. Electron images were recorded per projectile impact using a position sensitive detector/fast digital camera, and after processing the images the x–y coordinates of the impact were determined [6]. The secondary ions were detected using a microchannel-plate based multi-anode detector and were stored on a multi-channel time-to-digital converter (TDC). Materials for neat targets were obtained from Sigma Aldrich (St. Louis, MO). Surface target homogeneity was achieved by using vapor and electrospray deposition techniques. For electrospray depositions, samples were dissolved in 50% water/methanol solution. For photon experiments, all samples were deposited onto a 70–100 Ω/sq indium tin oxide coated glass (ITO/glass) substrate from Sigma Aldrich (St. Louis, MO). A sagittal rat brain section was used for secondary ion yield comparison purposes (courtesy of Dr. Amina S. Wood, NIDA, National Institute of Health, Baltimore, MD); details on the rat brain section preparation and extraction can be found elsewhere [7].

Experimental results show that the impact of an energetic C_{60} or Au_{400} projectile on a target surface induces a strong electronic excitation of the impacted volume ($\sim 10^3$ nm^3) and ionized ejecta. At the single impact level, photon, electron and secondary ion co-emission is observed, where their abundances increase with the projectile energy [8]. Time-resolved photon spectra of a series of targets (e.g., ionic salts, small dyes, small fluorophores and fluorophore label proteins) show that in the case of cluster projectiles the photon emission can be described by a narrow Gaussian distribution (few ns width) with a very short time decay in contrast to longer decays observed with monatomic and small polyatomic projectiles [9]. A comparison of the time-resolved photon spectra obtained from C_{60} and Au_{400} projectile is shown in Fig. 2 for the

* Corresponding author.
E-mail address: ffernandez@chem.tamu.edu (F.A. Fernandez-Lima).

0168-583X/$ - see front matter © 2011 Elsevier B.V. All rights reserved.
doi:10.1016/j.nimb.2011.07.092

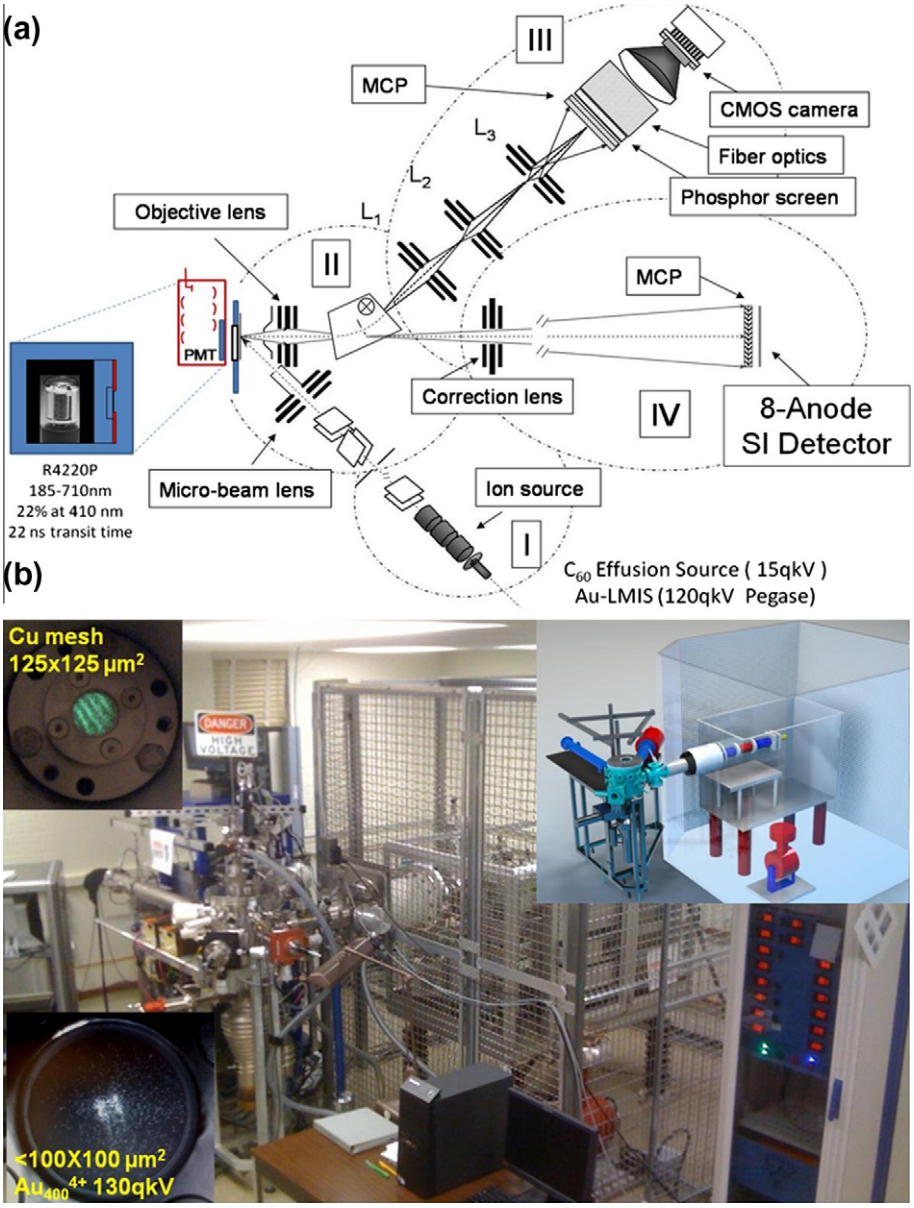

Fig. 1. (a) Schematics of the instrumental setup used for the detection of co-emitted photons, electrons and secondary ions from a single projectile impact. (b) Image of the Pegase 120 qkV Platform (Au-LMIS) coupled to the analysis chamber. In b, top and bottom insets of electron images as seen in the EEM phosphor screen for a continuous Au_{400} beam are shown.

case of a CsI/ITO target. In the case of C_{60}, we attribute the two fast components to the hollow nature of the projectile, which dissociates after penetrating a few layers and induces collision cascades involving projectile constituents and surface atom targets. A single component, fast photon emission is observed under massive gold projectile impacts associated with the projectile coherent motion. For the cases studied to date, the photon emission is target specific and increases with the projectile energy.

Multiple electron emissions are observed from a single impact, which enables the determination of the x–y coordinates of the impact site. Electron emission depends on the target composition, morphology and structure. For example, we have recently shown that the number of electrons emitted per C_{60} impact increases from organics to semiconductors to metals to ionic salts [5]. Moreover, we have also observed differences in the number of electrons from targets of similar composition (e.g., between bulk Al oxide, 50 nm Al oxide particles and 2 nm Al bohemite whiskers) and from single layer vs multi-layer nano-structures [10]. The cluster size and energy also affect the number of electrons emitted. As an example, electron distributions from a Glycine target bombarded by individual C_{60} and Au_{400} cluster projectiles are shown in Fig. 3. The electron distributions follow a Poisson distribution, analogous to those observed from atomic ion bombardment [11,12]. A significant feature is that in the case of C_{60} and Au_{400} cluster bombardment, electron emission is observed where kinetic electron emission from comparable velocity atomic projectiles does not occur [13,14]. Moreover, due to C_{60} and Au_{400} charge states (q = 1, 2 and q = 1–4, respectively), the phenomenon cannot be attributed to potential electron emission mechanism. That is, the unexpected electron emission under individual cluster bombardment is related to a collective effect during the projectile impact. Our results suggest that electronic excitations at the impact site are responsible for the coincidental electron and photon emission, both being characteristic of the target.

The unique feature of positional mass spectrometry is the ability to identify ions co-emitted from a single projectile impact. This

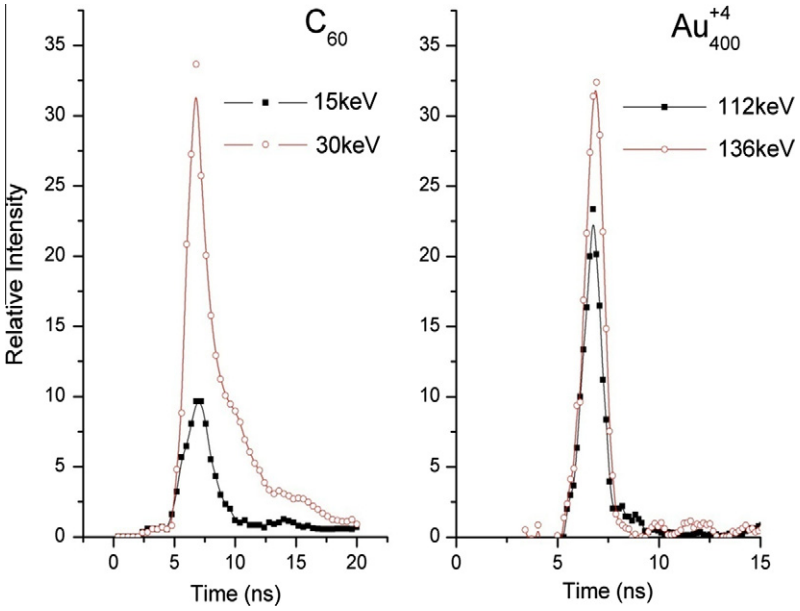

Fig. 2. Time-resolved photon spectra from a CsI/ITO target bombarded with (left) C_{60} and (right) Au_{400} projectiles.

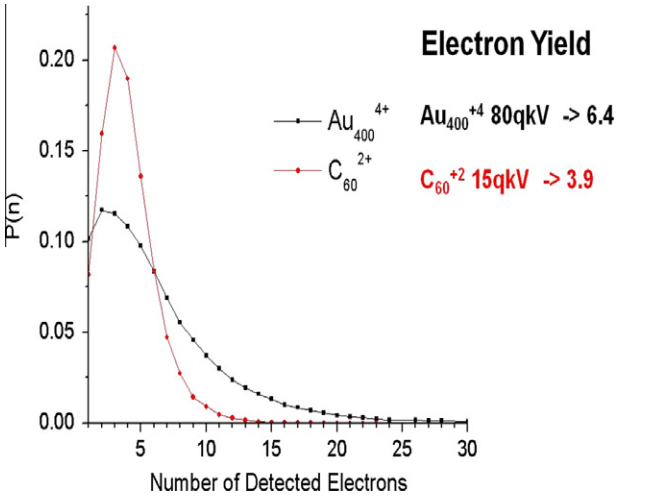

Fig. 3. Electron distributions from a Glycine target bombarded by individual C_{60} and Au_{400} cluster projectiles.

Table 1
Absolute secondary ion yields as a function of the projectile size and energy for a series of model biological surfaces (single component) and native biological surfaces (rat brain sections). Data are not corrected for detection efficiency; they are only corrected for transmission efficiency.

Target	*m/z*	Au_3^+ 50 keV	C_{60}^{+2} 43 keV	Au_{400}^{+4} 520 keV
CsI target	127	3.84E−01	6.56E−01	14.59
CsI target	387	1.61E−01	7.35E−01	12.54
Model biological surfaces				
Glycine CN^-	26	1.08E−01	2.12E−01	4.55
Glycine M^-	75	8.87E−01	4.57E−01	3.04
PG18:0–18:1 PO_3^-	79	1.56E−01	2.75E−01	4.08
PG18:0–18:1 M^-	775	5.23E−03	3.14E−02	2.53E−01
YGGFL CN^-	26	6.64E−02	4.08E−1	5.26
YGGFL M^-	554	1.08E−02	7.55E−3	5.74E−01
Ang III CN^-	26	7.85E−02	1.32−E	4.59
Ang III M^-	929	1.06E−03	6.19E−3	1.54
Native biological surfaces				
CN^-	26	2.76E−02[1]	7.89E−02	3.67
PO_3^-	79	2.77E−01[1]	2.55E−01	3.11
Lipid 1 PI38:4/ST24:1	885.5	7.27E−03[1]	7.05E−03	1.41E−01
Lipid 2 ST24:0(OH)	906.6	4.17E−03[1]	3.27E−03	1.50E−01

[1] Data correspond to Au_3^+ at 130 keV.

information is spatially resolved in the size of the area of co-emission. As an example, total secondary ion and specific ion maps are shown in Fig. 4 for a CsI coated 400 mesh grid. An important feature of surface mapping is that the number of secondary ion per impact has to be significant. For the case of atomic and poly-atomic ions, due to lower secondary ion yields, this approach is mainly limited to low mass secondary ions (e.g., atomic ions and small fragments). Nevertheless, due to the high desorption yields observed with cluster ions, surface mapping of molecular ions can be attainable from single impacts and from undamaged areas.

A comparison of secondary ion yields from model and native biological targets can be found in Table 1 for: (i) 50 keV Au_3^+ (equivalent to commercially available 50 keV Bi_3^{+2}), (ii) C_{60} and (iii) massive Au_{400}^{+4} projectiles. As a general trend, higher secondary ion emission and reduced fragmentation are observed for C_{60} and Au_{400}^{+4} relative to Au_3^{+1} projectiles. Previous studies have shown that for small gold cluster projectiles (e.g., Au_3^+), the secondary ion emission from organic samples reaches a maximum around 30–40 keV/atom [15]. The analysis of native biological samples shows that 130 keV Au_3^+ secondary ion yields are one and two orders lower when compared to 130 keV Au_9^+ and 520 keV Au_{400}^{+4}, respectively. A similar trend has been observed for biomolecular solids [16]. In the case of cluster projectiles, C_{60}, we have previously shown that the secondary ion yield increases with the projectile energy (15–43 keV) [8]. For massive 300–520 keV Au_{400}^{+4} projectiles, multiple atomic and small fragment ions are observed per projectile impact (yield > 1 per nominal mass); moreover, molecular ion yields of few tens of percent are obtained from model targets (single component) and few percents from native biological surfaces in the $500 < m/z < 1500$ mass range [17].

These results show the advantage of individual cluster impacts for surface characterization in comparison with atomic and poly-atomic beam techniques. The event-by-event bombardment-detection localization mode offers as a unique feature the combined characterization of a target surface using co-emitted photons, electrons and secondary ions; this information can later be

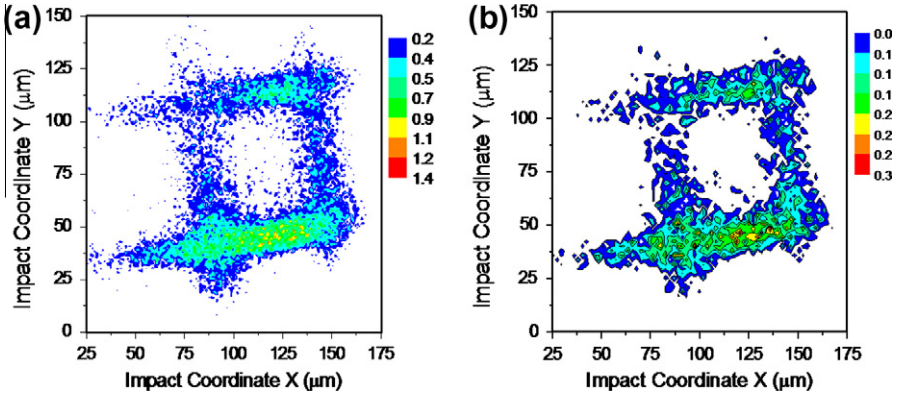

Fig. 4. (a) Total secondary ion and (b) $(CsI)I^-$ ion specific maps obtained from a CsI coated 400 mesh grid.

used as a surface fingerprint for target composition, morphology and structure. This approach is promising for molecular ion mapping at the nanoscale level with large applications in materials science, as well as biological and nanotechnology studies.

Acknowledgments

This work was supported by the National Science Foundation (Grant CHE-0750377). F. A. F-L acknowledges the National Institute of Health support (Grant No. 1K99RR030188-01). We will also like to thank Dr. Amina S. Wood for her insights and support.

References

[1] N. Winograd, Z. Postawa, J. Cheng, C. Skazal, J. Kozole, B.J. Garrison, Improvements in SIMS continue: is the end in sight?, Appl Surf. Sci. 252 (2006) 6836.
[2] S.V. Verkhoturov, R.D. Rickman, C. Guillermier, G.J. Hager, J.E. Locklear, E.A. Schweikert, Molecular ion emission from single large cluster impacts, Appl. Surf. Sci. 252 (2006) 6490.
[3] A. Tempez, J.A. Schultz, S. Della-Negra, J. Depauw, D. Jacquet, A. Novikov, Y. Lebeyec, M. Pautrat, M. Caroff, M. Ugarov, H. Bensaoula, M. Gonin, K. Fuhrer, A. Woods, Orthogonal time-of-flight secondary ion mass spectrometric analysis of peptides using large gold clusters as primary ions, Rapid Commun. Mass Spectrom. 18 (2004) 371.
[4] S. Della-Negra, J. Arianer, J. Depauw, S.V. Verkhoturov, E.A. Schweikert, The Pegase project, a new solid surface probe: focused massive cluster ion beams, Surf. Interface Anal. 43 (2011) 66.
[5] S.V. Verkhoturov, M.J. Eller, R.D. Rickman, S. Della-Negra, E.A. Schweikert, Single impacts of C60 on solids: emission of electrons, ions and prospects for surface mapping, J. Phys. Chem. C 114 (2009) 5637.
[6] M.J. Eller, S.V. Verkhoturov, S. Della-Negra, R.D. Rickman, E.A. Schweikert, Real-time localization of single C_{60} impacts with correlated secondary ion detection, Surf. Interface Anal. 43 (2011) 484.
[7] B. Colsch, A.S. Woods, Localization and imaging of sialylated glycosphingolipids in brain tissue sections by MALDI mass spectrometry, Glycobiology 20 (2010) 661.
[8] F.A. Fernandez-Lima, M.J. Eller, S.V. Verkhoturov, S. Della-Negra, E.A. Schweikert, Photon, electron and secondary ion emission from single C_{60} keV impacts, J. Phys. Chem. Lett. 1 (2010) 3510.
[9] F.A. Fernandez-Lima, V.T. Pinnick, S. Della-Negra, E.A. Schweikert, Photon emission from massive projectile impacts on solids, Surf. Interface Anal. 43 (2011) 53.
[10] M.J. Eller, S.V. Verkhoturov, S. Della-Negra, E.A. Schweikert, Electron emission from hypervelocity C_{60} impacts, J. Phys. Chem. C 114 (2010) 17191.
[11] K.H. Krebs, Secondary electron release at metal surfaces due to positive molecular ions, Ann. Phys. 13 (1964) 97.
[12] H.P. Winter, M. Vana, C. Lemell, F. Aumayr, Interaction of slow multicharged ions with solid surfaces: current concepts and new information on slow electron emission, Nucl. Instrum. Methods. Phys. Res. Sect. B: Beam Interact. Mater. Atoms 115 (1996) 224.
[13] A. Brunelle, P. Chaurand, S. Della-Negra, Y.L. Beyec, E. Parilis, Secondary electron emission yields from a CsI surface under impacts of large molecules at low velocities (5×10^3–7×10^4 ms^{-1}), Rapid Commun. Mass Spectrom. 11 (1997) 353.
[14] F. Aumayr, G. Betz, T.D. Mark, P. Scheier, H.P. Winter, Electron emission from a clean gold surface bombarded by slow multiply charged fullerenes, Int. J. Mass Spectrom. 174 (1998) 317.
[15] A. Brunelle, S. Della-Negr, J. Depauw, D. Jacquet, Y. Le Beyec, M. Pautrat, K. Baudin, H.H. Andersen, Enhanced secondary-ion emission under gold-cluster bombardment with energies from keV to MeV per atom, Phys. Rev. A 63 (2001) 022902.
[16] A. Novikov, M. Caroff, S. Della-Negra, J. Depauw, M. Fallavier, Y. Le Beyec, M. Pautrat, J.A. Schultz, A. Tempez, A.S. Woods, The Aun cluster probe in secondary ion mass spectrometry: Influence of the projectile size and energy on the desorption/ionization rate from biomolecular solids, Rapid Commun. Mass Spectrom. 19 (2005) 1851.
[17] F.A. Fernandez-Lima, J. Post, J.D. DeBord, M.J. Eller, S.V. Verkhoturov, S. Della-Negra, A.S. Woods, E.A. Schweikert, Analysis of native biological surfaces using a 100 kV massive gold cluster source, Anal. Chem., submitted for publication.